PLoS one

Identification of a PA-Binding Peptide with Inhibitory Activity against Influenza A and B Virus Replication

Kerstin Wunderlich[1,9], Daniel Mayer[1,9], Charlene Ranadheera[2,3], Anne-Sophie Holler[1], Benjamin Mänz[1], Arnold Martin[1], Geoffrey Chase[1], Werner Tegge[4], Ronald Frank[4], Ulrich Kessler[2], Martin Schwemmle[1]*

1 Department of Virology, University of Freiburg, Freiburg, Germany, 2 PiKe Pharma GmbH, Zurich, Switzerland, 3 Institute of Pharmaceutical Sciences, Swiss Federal Institute of Technology (ETH), Zurich, Switzerland, 4 Department of Chemical Biology, Helmholtz Centre for Infection Research, Braunschweig, Germany

Abstract

There is an urgent need for new drugs against influenza type A and B viruses due to incomplete protection by vaccines and the emergence of resistance to current antivirals. The influenza virus polymerase complex, consisting of the PB1, PB2 and PA subunits, represents a promising target for the development of new drugs. We have previously demonstrated the feasibility of targeting the protein-protein interaction domain between the PB1 and PA subunits of the polymerase complex of influenza A virus using a small peptide derived from the PA-binding domain of PB1. However, this influenza A virus-derived peptide did not affect influenza B virus polymerase activity. Here we report that the PA-binding domain of the polymerase subunit PB1 of influenza A and B viruses is highly conserved and that mutual amino acid exchange shows that they cannot be functionally exchanged with each other. Based on phylogenetic analysis and a novel biochemical ELISA-based screening approach, we were able to identify an influenza A-derived peptide with a single influenza B-specific amino acid substitution which efficiently binds to PA of both virus types. This dual-binding peptide blocked the viral polymerase activity and growth of both virus types. Our findings provide proof of principle that protein-protein interaction inhibitors can be generated against influenza A and B viruses. Furthermore, this dual-binding peptide, combined with our novel screening method, is a promising platform to identify new antiviral lead compounds.

Introduction

Influenza A and B viruses are closely related RNA viruses, which cause respiratory disease in humans and other animals. Both viruses belong to the Orthomyxoviruses, a family of enveloped, negative-sense RNA viruses that encode their genetic information in eight segments. While influenza A viruses (FluA) infect a broad variety of animals as well as humans, influenza B viruses (FluB) are predominantly found in humans [1]. Recently, FluA viruses have attracted the world's attention due to their ability to cause global pandemics, such as the 1918 "Spanish" flu or the novel H1N1 influenza virus of swine origin [2,3,4]. However, both FluA and FluB viruses are responsible for seasonal epidemics, which result in hundreds of thousands of deaths each year, since FluB can cause the same spectrum of symptoms that is observed with FluA [5,6,7,8,9]. In most years, only one type causes the majority of the cases, leading to the exclusion of the others [1]. For this reason, the annual influenza vaccination recommended by the WHO contains both FluA and FluB strains (http://www.who.int/csr/disease/influenza/vaccinerecommendations1/en/). Thus, both types A and B viruses pose a large threat to public health.

Since the current vaccines against influenza viruses offer only incomplete protection, antivirals are greatly needed. Presently, the only class of anti-influenza drugs available which are active against both FluA and FluB are neuraminidase inhibitors oseltamivir (Tamiflu) and zanamivir (Relenza) [10]. However, many influenza A strains, including the circulating H1N1 strains in Europe and the US, are already resistant to oseltamivir [11,12], suggesting a limited range of use for this type of drug. The resistance is not restricted to FluA, since the emergence of FluB viruses with reduced sensitivity to neuraminidase inhibitors is known [13,14]. In addition, the treatment of influenza B, particularly in young children, is associated with delayed antiviral effects and clinical resolution [15]. This might be related to the observation that oseltamivir carboxylate, the active metabolite of oseltamivir, is less active against the FluB rather than the FluA virus neuraminidase [13]. Other approved antivirals that target the viral M2 protein, such as amantadine, are only effective against FluA strains, since FluB strains lack a comparable M2 protein [16]. Additionally, the high prevalence of resistance to M2 inhibitors and the general rapid appearance of resistant strains during treatment restricts the therapeutic potential of this class of antiviral drugs [17].

Influenza virus replication and transcription is performed in the nucleus by the heterotrimeric viral polymerase complex consisting of the PB1, PB2, and PA subunits. This includes the synthesis of the genomic RNA from an intermediate copy RNA and the synthesis of viral mRNA transcripts. Synthesis of the latter transcripts is dependent on 8–15 nt long primers derived from the 5′ends of capped endogenous mRNAs. PB1 possesses the RNA polymerization activity, whereas PB2 is known to bind capped mRNA [18,19,20]. Recently, RNAse activity could be identified in the N-terminal part of PA, which is most likely necessary to cleave the primer off the remaining host mRNA [21,22]. The structure of the trimeric complex at the atomic level is not yet resolved, but cryo-EM studies do exist [23,24]. Recent crystal structures have shown that PB1 binds to PA via a 3_{10}-helix at its N-terminus comprised of amino acids (aa) 5–11 [25,26]. This finding is compatible with previous observations that the PA-binding site is localized to the extreme N-terminus of PB1 [27,28]. Since the association of these subunits is essential for viral replication [28,29,30,31], and since the sequence of this domain of PB1 is highly conserved among FluA strains [32], this interaction presents an attractive target for antiviral drugs. We have previously shown that a peptide derived from the first 25 amino acids of FluA PB1 can inhibit both the polymerase activity and viral spread of FluA but not FluB [32]. Here, we identify a chimeric FluA/FluB peptide which is active against both virus types.

Results

The type-specificity of the PA-PB1 interaction is due to the first 25 amino acids of PB1

Previously, we have shown that the N-terminal 25 aa of FluA PB1 ($PB1_{1-25}A$) are sufficient to bind FluA-PA and inhibit the polymerase activity of FluA [32]. However, this sequence was not able to block the polymerase activity of FluB. Since the first 25 aa of FluA-PA and FluB-PA differ at 8 positions (Fig. 1A), the failure to block FluB polymerase activity might be due to impaired binding of $PB1_{1-25}A$ to FluB PA. Alternatively, the PA-binding domain of FluB PB1 might extend beyond the extreme 25 amino
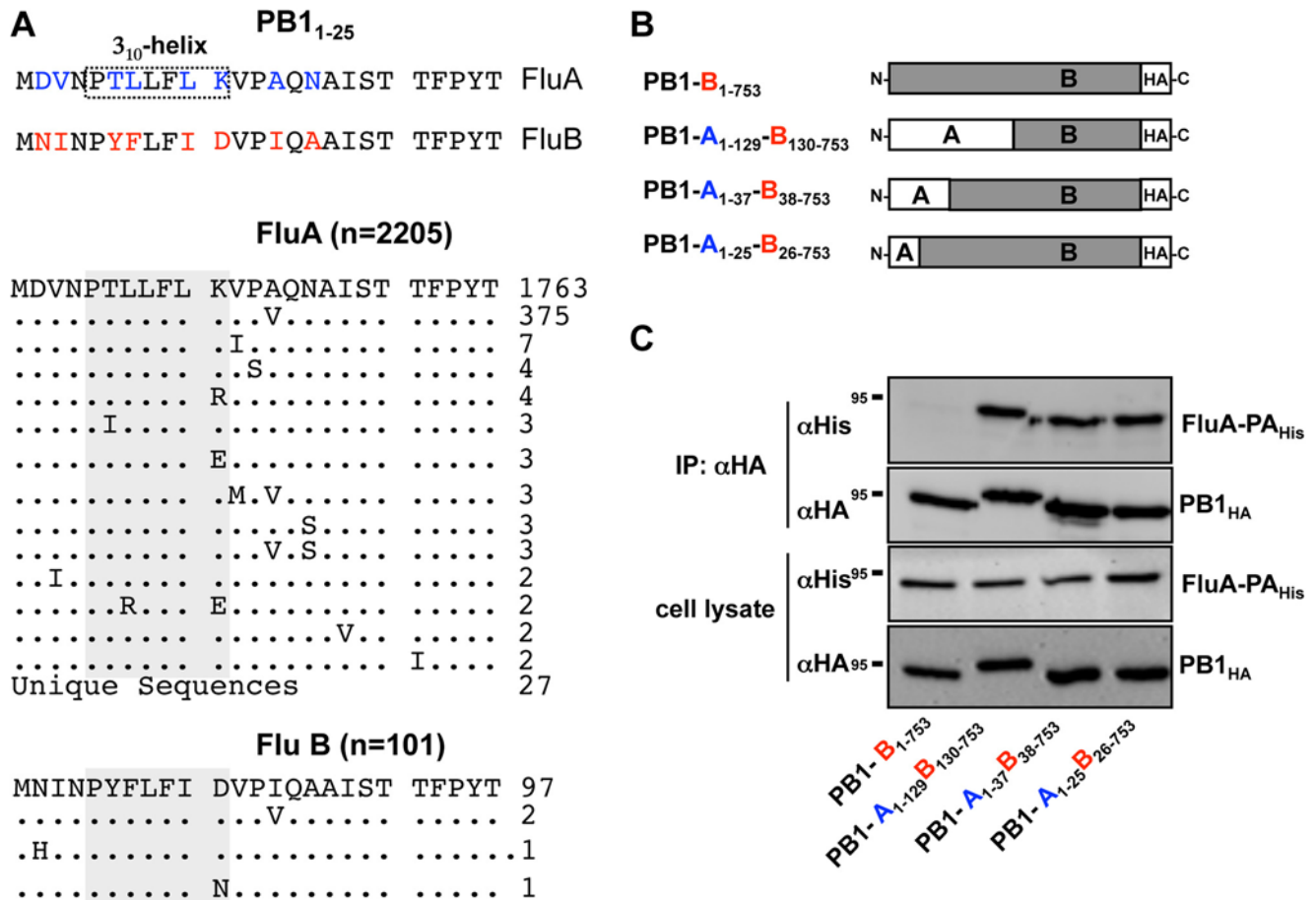

Figure 1. Virus type-specific conservation of the PA-binding domain and interaction of PA with PB1. (A) Upper panel: Alignment of the N-terminal 25 aa of FluA and FluB PB1. The dotted box indicates the 3_{10}-helix comprising the core PA-binding domain of PB1. FluA-specific (blue) and FluB-specific (red) aa are highlighted. Middle and lower panels: Alignment of the N-terminal 25 aa of all available FluA and FluB sequences available in the NCBI influenza virus database. Figures on the right hand side indicate the number of sequences present in the database. Grey bars highlight aa which reconstitute the 3_{10}-helix of FluA PA and possibly of FluB PA. (B) A/SC35M- and B/Yamagata/73-derived PB1 chimeras used in (b). Note that all PB1 proteins were expressed with C-terminal HA-tags. (C) Human 293T cells were transfected with expression plasmids coding for the indicated PB1 proteins and the C-terminally hexahistidine-tagged PA of FluA (FluA-PA$_{His}$). Cell lysates were prepared 24 hours post transfection and subjected to immunoprecipitation (IP) using anti-HA (αHA) agarose. Precipitated material was separated by SDS-PAGE and analyzed by Western blot for the presence of either His- or HA-tagged polymerase subunits using appropriate antibodies. Protein expression was controlled by analyzing equal amounts of cell lysate. Molecular weights are shown in kilodaltons.
doi:10.1371/journal.pone.0007517.g001

acids. To test this, we generated FluA/B PB1 chimeras by substituting N-terminal regions of varying length from FluA-PB1 into FluB-PB1 (Fig. 1B). After transient co-expression in human 293T cells, we then used immunoprecipitation assays to test which of these chimeras could bind to FluA-PA. All PB1 chimeras tested, including a chimera containing only the first 25 aa of FluA-PB1, could bind FluA-PA equally, whereas wild-type FluB-PB1 could not (Fig. 1C). This implied that the few aa differences in this small domain are the major determinant in PB1 for the type-specific binding of PB1 to PA.

Quantification of the PA/PB1 interaction

To further characterize which amino acid positions are important for the type-specific binding of $PB1_{1-25}$ to PA, we developed an ELISA-based binding assay to quantify this interaction. For this purpose, we immobilized biotinylated peptides corresponding to $PB1_{1-25}$ on streptavidin-coated plates and subsequently added cell lysates containing HA-tagged PA. Bound PA was detected using HA-specific primary and perox-idase-coupled secondary antibodies. To determine the binding efficiency of variant peptides we performed the ELISA in a competitive manner. In this case, non-biotinylated competitor peptides were added simultaneously with HA-tagged PA to wells containing immobilized $PB1_{1-25}$ peptide.

The core-binding site of the PA-binding domain of FluA-PB1 was recently determined by co-crystallization with the C-terminus of PA and is comprised of a 3_{10}-helix ranging from aa 5–11 [25]. We therefore first evaluated our FluA-binding assay by using a soluble wild-type $PB1_{1-25}A$ peptide, which resulted in a 50% inhibitory concentration (IC_{50}) of 1.8 nM (Fig. 2A). A "scrambled peptide" harboring the same amino acid composition as $PB1_{1-25}A$ but with the order randomized, did not block PA-HA binding at highest concentrations (3000 nM, data not shown). Next, the minimal binding domain was determined by deleting aa from the N- and/or C-terminus of PB11-25A. Determination of the IC_{50} using the truncated competitor peptides demonstrated that the 3-10 helix is absolutely essential for binding to PA, since any truncation of this sequence resulted in no competition (Fig. 2B). This is congruent with the results obtained by mutational analysis of the PA-binding domain [28]. Residual competition from partially C- or N-truncated peptides was observed, implying that some of the aa positions flanking the 3–10 helix may be dispensable for binding. Specifically, truncating the C-terminal 10 aa of FluA $PB1_{1-25}A$ resulted in an IC_{50} of 43.3 nM compared to 1.8 nM for the full-length peptide (Fig. 2B). Since this truncated peptide can efficiently bind to PA, yet still contains many of the differing aa positions between FluA and FluB, we chose this sequence as a basis to test variant peptides for their binding to both FluA- and FluB-PA.

A single amino acid substitution allows PB11-25 to bind FluA PA and FluB PA

As the $PB1_{1-15}$ sequence differs by 8 aa between FluA and FluB (Fig. 1A), we decided to create chimeras containing combinations of FluA- and FluB-specific residues and test these 15mer peptides in the competitive ELISA using both FluA-PA and FluB-PA. For this assay, biotinylated $PB1_{1-25}A$ was used in combination with FluA-PA-HA, biotinylated $PB1_{1-25}B$ was combined with FluB-PA-HA, and the competitor peptides were tested with both combinations. Competitor peptides $PB1_{1-15}A$ and $PB1_{1-15}B$, derived from the wild-type sequences, competed only for FluA PA or FluB PA, respectively, with no cross-type competition detectable (Fig. 3). We then tested competitor peptides containing combinations of FluB-specific aa in the $PB1_{1-15}A$ background. While most of these

combinations showed no affinity for FluB, substituting positions 6 and 7 led to a significantly reduced IC_{50} for FluB-PA as well as a slight decrease in the IC_{50} for FluA-PA, suggesting that this peptide could bind to both proteins. By substituting only the FluB-specific tyrosine at position 6, efficient binding to PA of both types resulted. In contrast, changing only position 7 of a FluA- to a FluB-specific sequence ablated binding to PA of both types. Introduction of a phenylalanine or tryptophan at position 6 demonstrated that related residues can significantly increase the binding affinity to FluA PA, but only partially increase the affinity to FluB PA. A histidine or cysteine at position 6 led to peptides failing to bind to FluB PA, while binding to FluA PA was still possible, indicating that not all amino acid substitutions confer the dual-binding activity observed with tyrosine at this position.
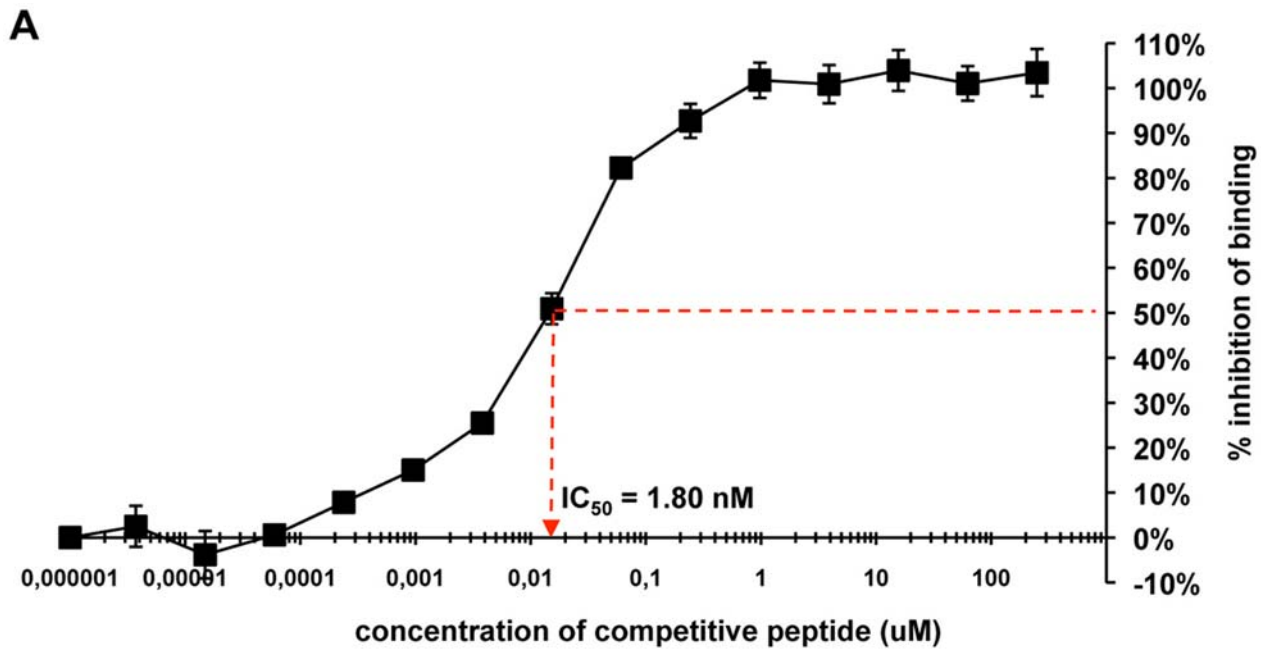
To further confirm that tyrosine at position 6 of FluA PB1 can bind directly to both FluA- and FluB-PA, we used a biotinylated 25mer peptide $PB1_{1-25}A_{T6Y}$ as well as wild-type peptides and cell lysates containing overexpressed PA-HA derived from several different FluA and FluB strains in the ELISA. As shown in Fig. 4A–C, PA-HA from several FluA strains of various subtypes, including a human H5N1 isolate, bound to both $PB1_{1-25}A$ and $PB1_{1-25}A_{T6Y}$, but not to $PB1_{1-25}B$ or a scrambled biotinylated peptide. Conversely, PA-HA derived from several different FluB strains bound to both the $PB1_{1-25}B$ and $PB1_{1-25}A_{T6Y}$ (Fig. 4D). Thus, a FluA-PB1-derived sequence containing a single substitution at position 6 can directly bind to PA from different FluA and FluB viruses. Molecular modeling suggests that the FluB-derived tyrosine at position 6 of $PB1_{1-25}A_{T6Y}$ fits into a hydrophobic pocket of FluA PA and displaces a water molecule (Fig. 3F). Both the increased hydrophobic interaction as well as the entropic effect of the water displacement might explain the enhanced binding of PB1-T6Y to PA of FluA and possibly of FluB.

$PB1_{1-25}A_{T6Y}$ can inhibit the polymerase activity and spread of FluA and FluB

To demonstrate that $PB1_{1-25}A_{T6Y}$ can bind to both FluA- and FluB-PA in a cellular context, we performed immunoprecipitation experiments using overexpressed PA and $PB1_{1-25}$ peptides fused to GFP (Fig. 5B). This confirmed that $PB1_{1-25}$ derived from FluA or FluB can only bind to FluA-PA or FluB-PA, respectively. However, $PB1_{1-25}A_{T6Y}$ could be immunoprecipitated with either FluA-PA or FluB-PA.

Next, we tested the ability of these fusion proteins to inhibit the polymerase activity of both FluA and FluB using a reconstituted viral ribonucleoprotein complex and a reporter gene. As previously shown [32], $PB1_{1-25}A$-GFP inhibits the activity of FluA, but not FluB, while the converse is true of $PB1_{1-25}B$-GFP (Fig. 5C). However, $PB1_{1-25}A_{T6Y}$-GFP inhibited both FluA and FluB polymerase activity to comparable levels as the wild-type-derived sequences (Fig. 5C), indicating that this variant peptide is also biologically active.

Finally, we tested the ability of these peptides to inhibit viral spread in cell culture. MDCK cells were infected with either A/WSN/33 (H1N1), A/Thailand/1/2004 (H5N1), B/Yamagata/73, or vesicular stomatitis virus (VSV) as a specificity control from a different virus family. A plaque reduction assay was then performed in the presence of $PB1_{1-25}A$, $PB1_{1-25}A_{T6Y}$, or a negative-control peptide fused to an HIV-Tat derived sequence [33] (Table 1) to allow the peptides to cross the plasma membrane. Similar experiments with a FluB-derived peptide were not possible due to its insolubility. The peptide containing the T6Y substitution inhibited the growth of all influenza strains tested, while $PB1_{1-25}A$-Tat only inhibited FluA (Fig 6). Thus, a single mutation in the $PB1_{1-25}A$ sequence results in a peptide which is active against both FluA and FluB strains.

Figure 2. Quantification of the interaction between PB1$_{1-25}$ and PA. (A) Determination of the 50% inhibitory concentration (IC$_{50}$) of PB1$_{1-25}$A by competitive ELISA using the indicated increasing concentrations of peptides and cell extract containing HA-tagged PA of FluA. Error bars represent standard deviations from triplicate experiments. (B) IC50 of PB1$_{1-25}$A-derived peptides. S.D. is shown in parenthesis. Asterisks indicate highest concentrations of peptides (3000 nM) used without detectable inhibitory effect. Grey boxes highlight amino acids that are part of the 3$_{10}$-helix, which was postulated to comprise the core PA-binding region of PB1. Amino acids known to form hydrogen bonds with PA residues are represented in bold.
doi:10.1371/journal.pone.0007517.g002

Competitive peptide		IC$_{50}$ (nM)	
		PA (FluA)	PA (FluB)
PB1$_{1-15}$ A	MDVNPTLLFLKVPAQ	43.32 (+/- 5.31)	>3000*
PB1$_{1-15}$ B	.NI..YF..ID..I.	>3000*	45.0 (+/-12.5)
PB1$_{1-15}$ A$_{D2N,V3I,L14I}$	.NI..........I.	6.69 (+/- 1.73)	>3000*
PB1$_{1-15}$ A$_{L10I,K11D}$	.........ID....	>3000*	>3000*
PB1$_{1-15}$ A$_{D2N,V3I}$	.NI............	12.96 (+/- 3.98)	>3000*
PB1$_{1-15}$ A$_{T6Y,L7F}$	.....YF........	7.51 (+/- 0.71)	345.0 (+/-81.5)
PB1$_{1-15}$ A$_{L7F}$	......F........	>3000*	>3000*
PB1$_{1-15}$ A$_{T6Y}$	.....Y.........	21.64 (+/- 1.48)	107.1 (+/-31.3)
PB1$_{1-15}$ A$_{T6F}$	.....F.........	2.84 (+/- 0.48)	750.4 (+/-249.6)
PB1$_{1-15}$ A$_{T6W}$	.....W.........	3.40 (+/- 0.51)	628.3 (+/-389.1)
PB1$_{1-15}$ A$_{T6H}$	.....H.........	292.16 (+/- 34.04)	>3000*
PB1$_{1-15}$ A$_{T6C}$	.....C.........	43.58 (+/- 5.67)	>3000*

Figure 3. Binding characteristics of FluA and FluB PB1-derived peptide chimera. Inhibitory concentrations of FluA/FluB-derived peptides determined by competitive ELISA. Competitor peptides (0.048 to 3000 nM) were mixed with cell extracts containing HA-tagged PA from either FluA or FluB. Letters in red indicate FluB, letters in blue FluA specific aa. S.D. is indicated in parenthesis. Asterisks indicate highest concentrations of peptides used without reaching 50% inhibition.
doi:10.1371/journal.pone.0007517.g003

Discussion

Here we report that the PA-binding domains of the polymerase subunits PB1 of influenza A and B viruses are highly conserved within each virus type, and that these domains are not mutually exchangeable. Based on phylogenetic analysis and a biochemical ELISA-based screening approach, we were able to identify a PB1-derived peptide of influenza A virus with a single influenza B-specific amino acid substitution which recognizes PA of both virus types. Significantly, this dual-binding peptide blocked both the polymerase activity and spread of both viruses and raises the exciting possibility of developing new antivirals that specifically interfere with the polymerase complex assembly of both viruses.

The inability of PB1$_{1-25}$A to efficiently bind to FluB-PA and vice versa strongly indicates that these PA-binding domains show limited functional compatibility between the two virus types. We speculate that this incompatibility is caused by an independent evolution of the FluA and FluB polymerase proteins. This is in accordance with a virus-type specific conservation of the PA-binding domain of PB1 (Fig. 1) and further highlighted by an overall aa identity of the viral polymerase subunits of less than 35% between FluA and FluB strains. Together, these differences may account for the failure to reconstitute an active trimeric polymerase complex by mixing FluA and FluB polymerase subunits ([34,35,36], unpublished results). However, both FluA and FluB viruses have a common origin [1]. Thus, it is not unexpected that the aa residues of PA which are in close contact with PB1$_{1-25}$ are conserved between FluA and FluB [25,26], indicating that the PA domain of both virus types bind PB1 in a similar fashion. This similarity might explain how one single amino acid substitution (T6Y) in PB1$_{1-25}$A is sufficient to allow binding to FluB-PA. Based on the available crystal structure of PA complexed with the N-terminus of PB1 and our modeling results with this dual-binding peptide PB1$_{1-25}$A$_{6Y}$ (Fig. 4F), we speculate that the tyrosine residue might exploit a hydrophobic pocket in the PB1-binding domain of FluB PA, thereby stabilizing the interaction. Such an occupation of a hydrophobic pocket may also be important to stabilize the interaction between PB1$_{1-25}$A$_{6Y}$ and FluB PA.

Both the identification of the FluA- and FluB-PA-binding peptide PB1$_{1-25}$A$_{T6Y}$ and our novel ELISA-based screening assay provide a unique platform for future screening of small molecules targeting the PB1/PA interaction of both virus types. Such inhibitors represent attractive new tools to disrupt a variety of protein-protein interactions (PPI) [37,38]. Initial attempts to identify PPI inhibitors were challenged by the large contact surfaces of protein-protein interfaces. However, the identification of a small subset of aa residues, such as the PA-binding domain of PB1 that contribute to most of the free energy of binding provide excellent targets. Recent screening approaches led to the identification of potent PPI inhibitors that block dimerization between the human protein double mutant 2 (HDM2) and a 15-residue a-helical region of the tumor suppressor p53 [39], the basic helix-loop-helix leucine zipper (bHLHZip) transcription factor Myc and Max [40] or the interaction between paxilin and the integrin a4 [41]. Proof-of-principle that viral protein interactions are also attractive targets for the generation of PPI inhibitors was first obtained with human papilloma virus [42] and herpes simplex virus type 1 (HSV-1) [43]. In the case of HSV-1, the interaction between the catalytic subunit of the HSV-1 polymerase (UL30) and its cofactor, the processivity factor UL42 was targeted. Similar to the interaction of PB1 and PA, the extreme 18 C-terminal residues of UL30 are sufficient to bind to UL42. Using a biochemical screening assay based on the specific interaction of this C-terminal peptide and UL42, several potent small molecule inhibitors were identified [43]. It is therefore reasonable to assume that PPI inhibitors that block the dimerization of PB1 and PA can also be identified using the newly established ELISA-based screening assay. Indeed, recent results indicate that this approach has the potential to identify PPI inhibitors that prevent viral polymerase activity and replication of both types of influenza viruses (Kessler et al., unpublished results). We believe that the PB1/PA interface is an excellent target for PPI inhibitors, because the PA-binding domain within the extreme N-terminus of PB1 is crucial for the interaction with PA, since PB1 mutants lacking this domain fail to interact with PA [28]. Using PB1$_{1-25}$A$_{6Y}$ and FluA PA for screening, we expect that some PPI inhibitors possess a high specificity against both influenza virus types. This is supported by our observations that PB1$_{1-25}$A$_{6Y}$ blocks the growth of FluA and FluB but not VSV.

Besides the PA/PB1 complex, other targets of influenza viruses have become attractive for the development of PPI inhibitors, including the interaction interface between PB2 and PB1, for which the crystal structure was recently solved [44]. Additionally, based on the crystal structure of a fragment of PB2 bound to the cap analog m7GTP [20], non-PPI inhibitors might become feasible that compete with cap-binding properties of PB2. Furthermore, the
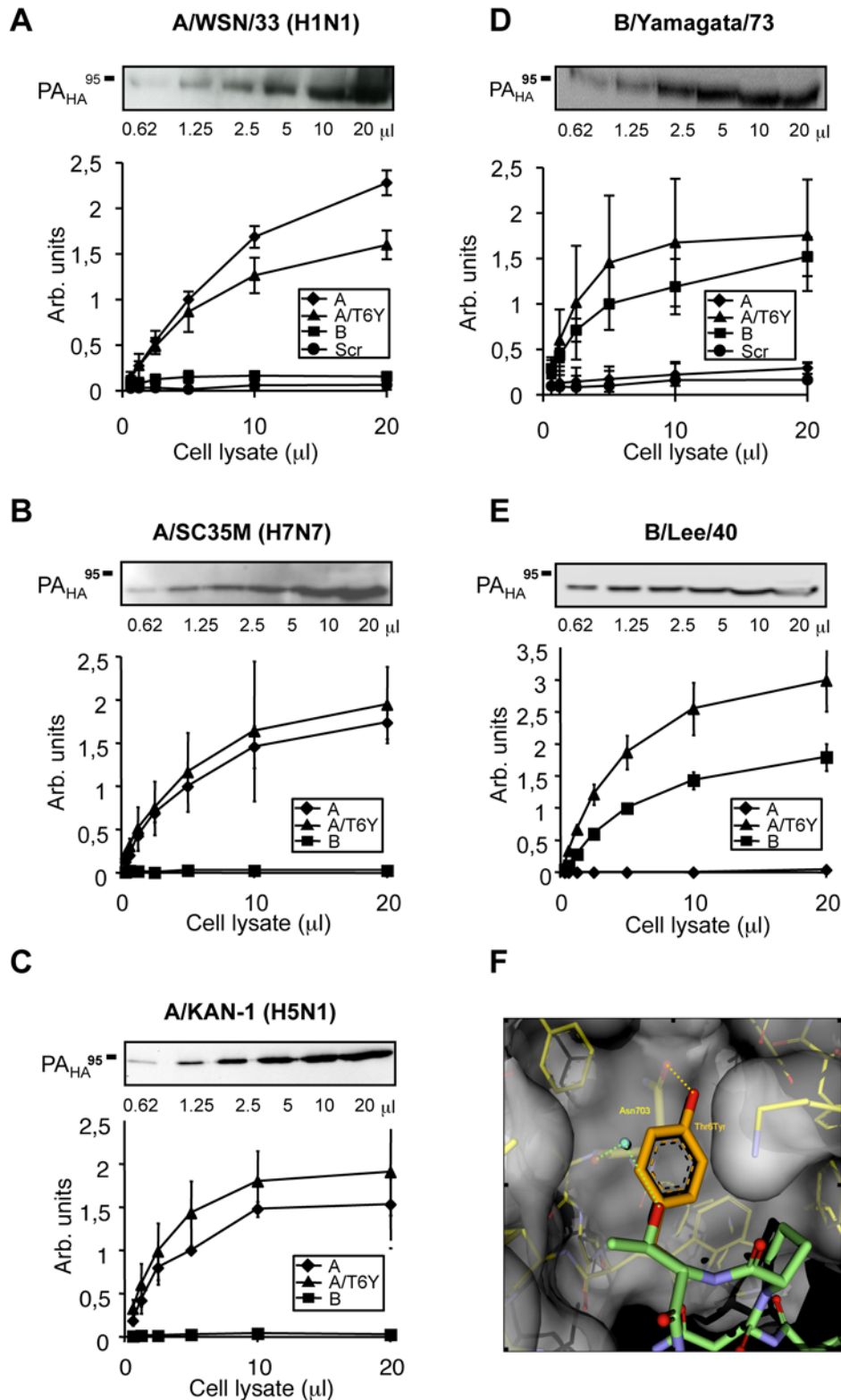
Figure 4. Dual-binding properties of the FluA/B peptide chimera PB1$_{1-25}$A$_{T6Y}$. (A) – (D) Binding of overexpressed HA-tagged PA subunits of differing influenza strains in cell extracts to the immobilized peptides corresponding to the domains of FluA PB1 (PB1$_{1-25}$A), FluB PB1 (PB1$_{1-25}$B) or FluA PB1 T6Y (PB1$_{1-25}$A$_{T6Y}$) was determined by ELISA. Signals using the cognate peptide and lysate were normalized to 1. Binding of the PA subunits to the control peptides was not observed (data not shown). Upper panels: Western blot of the PA-containing cell extracts used. Molecular weights shown in kilodaltons. (F) Structure of FluA PB1$_{1-15}$ (green) bound to FluA PA (grey) as published [25]. T6 forms a hydrogen bond (green line) to a water molecule (blue). Molecular modeling suggests that the aromatic side chain in the mutant T6Y (orange) fits into a hydrophobic pocket and displaces the water molecule.

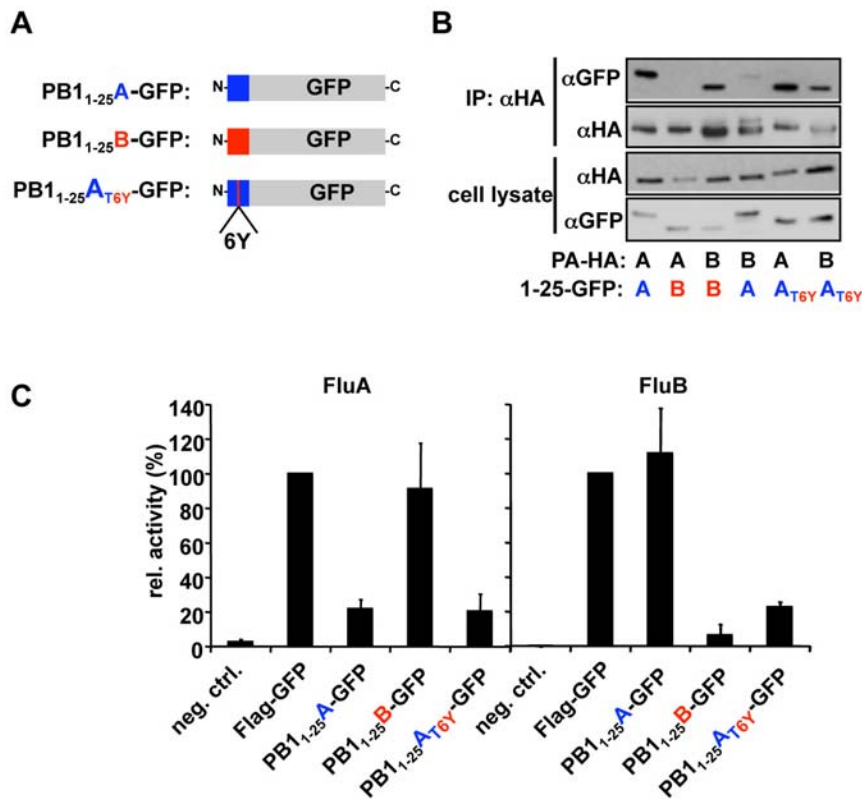doi:10.1371/journal.pone.0007517.g004

Figure 5. Virus-type independent binding and inhibition of GFP fused to the dual binding peptide PB1$_{1-25}$A$_{T6Y}$. (A) GFP-PB1 fusion proteins used in (B). (B) Complex formation of PB1$_{1-25}$-derived GFP fusion proteins and HA-tagged PA of FluA and FluB. Indicated proteins were expressed in human 293T cells and binding of the GFP fusion proteins was analyzed by IP using anti-HA agarose and subsequent immunoblotting. Precipitated material was visualized using the indicated antibodies for the presence of either HA-tagged PA or GFP. Molecular weights are shown in kilodaltons. (C) Polymerase inhibitory activity of PB1$_{1-25}$-derived GFP fusion proteins in FluA and FluB polymerase reconstitution assays. 293T cells were transiently transfected with a plasmid mixture containing either Flu A (A/WSN/33) or Flu B (B/Yamagata/73) PB1-, PB2-, PA- and NP-expression plasmids, polymerase I (Pol 1)-expression plasmid expressing an influenza virus-like RNA coding for the reporter protein firefly luciferase (FluA) or (FluB) to monitor viral polymerase activity and expression plasmids coding for the indicated GFP fusion proteins. The transfection mixture also contained a plasmid constitutively expressing renilla luciferase (100 ng), which served to normalize variation in transfection efficiency. The activity observed with transfection reactions containing Flag-GFP were set to 100%. The omission of PB2 in the transfection mixture served as a negative control.
doi:10.1371/journal.pone.0007517.g005

cap-snatching endonuclease of influenza virus polymerase localized in the N-terminal domain of PA [21,22] provides a further target for the development of effective inhibitors. However, it has yet to be shown whether these targets are suitable for the development of antivirals. Since the available information of these novel targets is restricted to FluA strains, it remains unclear whether such antivirals may also be active against FluB.

Attempts to substitute position 6 of the FluA PB1$_{1-25}$A peptides with other residues than tyrosine did not result in improved FluB-PA binding in the competitive ELISA experiments. However, replacements with either phenylalanine or tryptophan residues

enhanced binding to FluA-PA approximately 20 fold. This suggests that other substitutions may further enhance the binding affinity to FluA-PA and increases the antiviral activity of these peptides. In one study, random substitutions of single aa within an importin-alpha-binding peptide increased its affinity by several orders of magnitude [45], providing proof of principle that the development of potent peptide inhibitors from a peptide lead is possible. The antiviral activity of VIRIP, a peptide that blocks HIV-1 entry by interacting with the gp41 fusion peptide could be increased in its antiretroviral potency by two orders of magnitude [46]. Thus, random substitutions of the PA-binding domain may

Table 1. Peptides used for the plaque-reduction assay.

Peptide name	Peptide sequence
PB1$_{1-25}$A-Tat	MDVNPTLLFLKVPAQNAISTTFPYT***YGRKKRRQRRRPP***
PB1$_{1-25}$A$_{T6Y}$-Tat	MDVNP**Y**LLFLKVPAQNAISTTFPYT***YGRKKRRQRRRPP***
PX-Tat	LSNDELIKKLVTELAENSMIEAEEV***YGRKKRRQRRRPP***

The underlined Y highlights the tyrosine residue derived from the PB1 FluB sequence. Bold letters in italics represent the HIV-Tat derived sequence that allow the peptides to cross the plasma membrane.
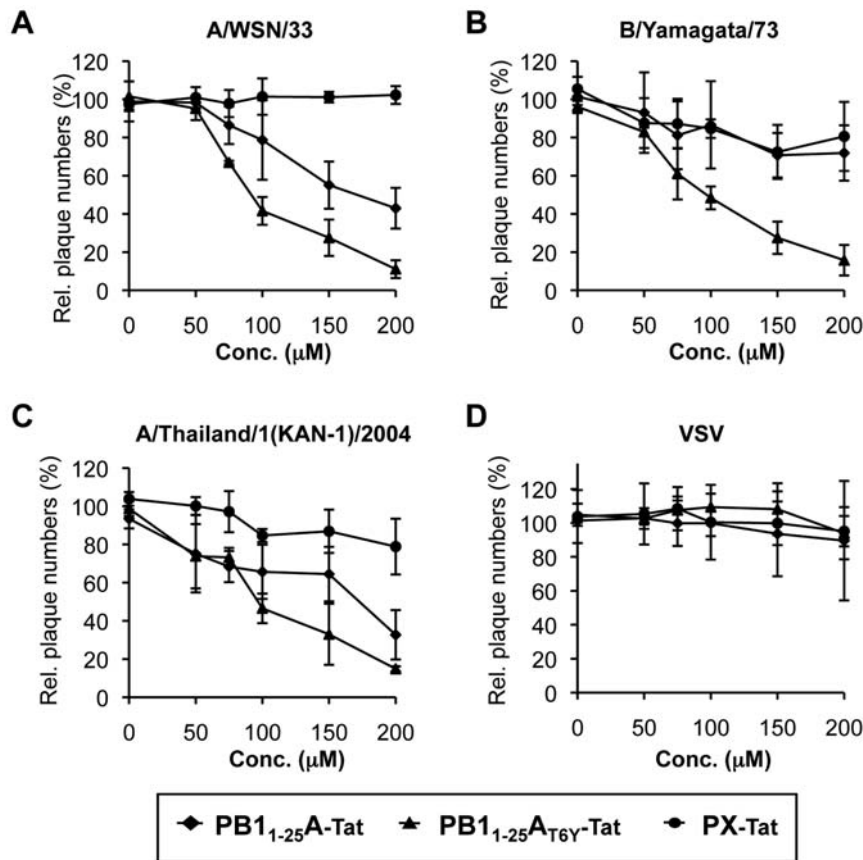doi:10.1371/journal.pone.0007517.t001

Figure 6. Inhibition of FluA and FluB by the dual binding peptide PB1$_{1-25}$A$_{T6Y}$. Plaque reduction assay using PB1$_{1-25}$A-Tat; PB1$_{1-25}$A$_{T6Y}$-Tat; PX-Tat (control peptide) [32] with FluA, FluB and VSV (vesicular stomatitis virus). A H$_2$O control was used to standardize the assay to 100%. Note that PB1$_{1-25}$B-Tat could not be tested due to insolubility. Error bars represent S.D.
doi:10.1371/journal.pone.0007517.g006

reveal peptides with significantly enhanced binding properties for FluA-PA. This approach might also lead to the identification of peptides, which bind PA of both virus types, using PB1$_{1-25}$A$_{6Y}$ as the lead peptide. Most importantly, such peptides would be prime candidates for the development of antiviral peptidomimetics.

Materials and Methods

Virus strains

Infection experiments were carried out using A/WSN/33 (H1N1) [32] and A/Thailand/1(Kan-1)/2004 [47], B/Yamagata/73 [48] and VSV (serotype Indiana) [49].

Plasmid constructions

Plasmids pCA-Flag-GFP and pCA-PB1$_{1-25}$A-GFP [32], pCA-PB1-HA [32], the FluA minireplicon plasmids [50] and the expression plasmids for the FluB minireplicon [32] were described elsewhere. The FluB minigenome expression plasmid, pPolI-lucRT_B, was obtained by cloning the firefly luciferase ORF (inverse orientation) flanked by the non-coding region of the segment 8 of the B/Yamagata/73 into the SapI-digested plasmid pPolI-SapI-Rib [50]. For the construction of pCA-PB1$_{1-25}$B-GFP, a linker containing the first 25 codons of PB1 (B/Yamagata/73) was cloned into the EcoRI/NotI sites of pCA-Flag-GFP plasmid, replacing the Flag-coding sequence with PB1$_{1-25}$B. Site directed mutagenesis was carried out with pCA-PB1$_{1-25}$A-GFP to create the plasmid pCA-PB1$_{1-25}$A$_{T6Y}$-GFP. The ORFs of PB1 (B/Yamagata/73) and PA

(A/SC35M, A/Thailand/1(KAN-1)/04, A/Vietnam/1203/04, B/Yamagata/73, B/Lee/40; accession numbers: Influenza A virus (A/WSN/1933(H1N1)) segment 2 (CY034138), segment 3 (CY034137), A/SC35M (H7N7) segment 2 (DQ266098), segment 3 (DQ266099), A/Thailand/1(KAN-1)/2004(H5N1) segment 3 (AY555150), B/Lee/40 segment 3 (NC_002206)) were PCR amplified with sense primers containing a NotI site (FluA strains) or a EcoRI site (FluB strains) upstream of the initiation codon and antisense primers with a deleted stop codon followed by an XmaI site, a coding sequence for an HA-tag and a XhoI site. The PCR products were cloned into a modified pCAGGs-vector [51] digested either with EcoRI/XhoI or NotI/XhoI, resulting in pCA-PB1-HA or pCA-PA-HA plasmids, coding for C-terminal tagged versions of the polymerase subunits. To obtain the pCA-PA$_{A/SC35M}$-His plasmid, pCA-PA$_{A/SC35M}$-HA was digested with XmaI/XhoI and the HA coding sequence was replaced by a 6xHis-linker. The A/B-chimeric expression plasmids were obtained by assembly PCR using the pCA-PB1-HA plasmids of SC35M and B/Yamagata/73 and by cloning the resulting PCR product in pCA-PB1$_{B/Yamagata/73}$-HA digested with EcoRI/EcoRV.

Reconstitution of the influenza virus polymerase activity

293T cells were transiently transfected with a plasmid mixture containing either FluA- or FluB-derived PB1-, PB2-, PA- and NP-expression plasmids, polymerase I (Pol I)-driven plasmid transcribing an influenza A or influenza B virus-like RNA coding for the reporter protein firefly luciferase to monitor viral polymerase activity and with expression plasmids coding for the indicated GFP

fusion proteins. Both minigenome RNAs were flanked by non-coding sequences of segment 8 of FluA and FluB, respectively. The transfection mixture also contained a plasmid constitutively expressing *Renilla* luciferase, which served to normalize variation in transfection efficiency. The reporter activity was determined 24 h post transfection and normalized using the Dual-Glu® Lufierase Assay System (Promega). The activity observed with transfection reactions containing Flag-GFP were set to 100%.

Peptide synthesis

The solid-phase synthesis of the peptides, including the peptides for the plaque reduction assay (Table 1), was carried out on a Pioneer automatic peptide synthesizer (Applied Biosystems, Foster City, USA) employing Fmoc chemistry with TBTU/diisopropyl-lethyl amine activation. Side chain protections were as follows: Asp, Glu, Ser, Thr and Tyr: t-Bu; Asn, Gln and His: Trt; Arg: Pbf; Lys and Trp: Boc. Coupling time was 1 h. Double couplings were carried out if a difficult coupling was expected according to the program Peptide Companion (CoshiSoft/PeptiSearch, Tucson, USA). All peptides were generated as carboxyl amides by synthesis on Rapp S RAM resin (Rapp Polymere, Tübingen, Germany). Biotin was incorporated at the C-terminus of indicated peptides with Fmoc-Lys(Biotin)-OH (NovaBiochem/Merck, Nottingham, UK) and TBTU/diisopropylethyl amine activation for 18 h, followed by coupling of Fmoc-β-Ala-OH for 1 h. Peptides were cleaved from the resin and deprotected by a 3 h treatment with TFA containing 3% triisobutylsilane and 2% water (10 ml/g resin). After precipitation with t-butylmethyl ether, the resulting crude peptides were purified by preparative HPLC (RP-18) with water/acetonitrile gradients containing 0.1% TFA and character-ized by analytical HPLC and MALDI-MS. Some peptides were synthesized by peptides&elephants (Nuthetal, Germany) and subsequently purified and characterized as described above.

Immunoprecipitation experiments

293T cells were transfected with the indicated plasmids in 6-well plates using Metafectene (Biontex, Martinsried, Germany). Cells were incubated 24 h post transfection with lysis buffer (20 mM Tris pH 7.5, 100 mM NaCl, 0.5 mM EDTA, 0.5% NP-40, 1% Protease inhibitor Mix G, (Serva, Heidelberg, Germany), 1 mM DTT) for 15 min on ice. After centrifugation by 13.000 rpm at 4°C supernatant was incubated with anti HA-specific antibodies coupled to agarose beads (Sigma) for 1 h at 4°C. After three washes with 1 ml of washing buffer (lysis buffer without protease inhibitor mix), bound material was eluted under denaturing conditions and separated on SDS-PAGE gels and transferred to PVDF membranes. Viral polymerase subunits and GFP fusion proteins were detected with antibodies directed against the HA-

(Covance, Berkeley, California) or His-(Qiagen) or GFP-tag (Santa Cruz Biotechnology).

Plaque reduction assay. The experiments were carried out as described [52] with modifications. Confluent MDCK cells were infected with **80 PFU of** A/WSN/33, B/Yamagata/73, A/KAN-1, or VSV/Indiana in PBS at room temperature. After removal of the inoculums, cells were overlaid with medium (DMEM with 20 mM Hepes) containing 1% Oxoidagar and peptides at the indicated concentrations. After incubation for 24 h (VSV), 48 h (A/WSN/33, A/KAN-1) at 37°C with 5% CO_2, or 72 h at 33°C with 5% CO_2 (B/Yamagata/73) respectively, cells were fixed with formaldehyde and stained with crystal violet. Plaques were counted and mean plaque number of the water control was set to 100%.

ELISA

Streptavidin-coated microwell plates were incubated with saturating concentrations of biotinylated peptides, washed and subsequently incubated at room temperature with HA-tagged PA. To obtain PA-HA, 293T cells were seeded into 94 mm-dishes, transfected with the respective plasmid and treated with lysis buffer 24 h post transfection as previously described [32]. After washing the microwell plates, the wells were incubated with an HA-specific primary antibody (Covance, MMS-101R), followed by three washes and an incubation with a peroxidase-coupled secondary antibody (Jackson Immuno Research, Newmarket, UK). After the final wash step, ABTS-substrate (Sigma, ready-to-use solution) was added and the optical density was determined at 405 nm.

The competition ELISA was carried out as described above with the exception that the competitor peptides were added to wells of the plate with bound peptides simultaneously with the addition of the cell extract containing HA-tagged PA subunits.

Sequence alignment. Alignments were performed with MUSCLE [53] using the full-length sequences provided from the public influenza virus database (http://www.ncbi.nlm.nih.gov/genomes/FLU/FLU.html).

Modeling. Manual docking of the mutated peptide into the PA(C)-PB1(N) crystal structure [25] and subsequent minimization was performed with Accelrys Discovery Studio.

Author Contributions

Conceived and designed the experiments: KW DM UK MS. Performed the experiments: KW DM CR ASH BM AM GC. Analyzed the data: KW DM CR ASH UK MS. Contributed reagents/materials/analysis tools: WT RF MS. Wrote the paper: UK MS.

References

1. Chen R, Holmes EC (2008) The evolutionary dynamics of human influenza B virus. J Mol Evol 66: 655–663.
2. Tumpey TM, Belser JA (2009) Resurrected Pandemic Influenza Viruses. Annu Rev Microbiol.
3. Parrish CR, Kawaoka Y (2005) The origins of new pandemic viruses: the acquisition of new host ranges by canine parvovirus and influenza A viruses. Annu Rev Microbiol 59: 553–586.
4. Neumann G, Noda T, Kawaoka Y (2009) Emergence and pandemic potential of swine-origin H1N1 influenza virus. Nature 459: 931–939.
5. Baine WB, Luby JP, Martin SM (1980) Severe illness with influenza B. Am J Med 68: 181–189.
6. Kim HW, Brandt CD, Arrobio JO, Murphy B, Chanock RM, et al. (1979) Influenza A and B virus infection in infants and young children during the years 1957-1976. Am J Epidemiol 109: 464–479.
7. Wright PF, Bryant JD, Karzon DT (1980) Comparison of influenza B/Hong Kong virus infections among infants, children, and young adults. J Infect Dis 141: 430–435.
8. Clark PS, Feltz ET, List-Young B, Ritter DG, Noble GR (1970) An influenza B epidemic within a remote Alaska community. Serologic, epidemiologic, and clinical observations. JAMA 214: 507–512.
9. Nolan TF, Jr., Goodman RA, Hinman AR, Noble GR, Kendal AP, et al. (1980) Morbidity and mortality associated with influenza B in the United States, 1979-1980. A report from the Center for Disease Control. J Infect Dis 142: 360–362.
10. Moscona A (2005) Neuraminidase inhibitors for influenza. N Engl J Med 353: 1363–1373.
11. Moscona A (2009) Global transmission of oseltamivir-resistant influenza. N Engl J Med 360: 953–956.
12. Dharan NJ, Gubareva LV, Meyer JJ, Okomo-Adhiambo M, McClinton RC, et al. (2009) Infections with oseltamivir-resistant influenza A(H1N1) virus in the United States. JAMA 301: 1034–1041.
13. Hatakeyama S, Sugaya N, Ito M, Yamazaki M, Ichikawa M, et al. (2007) Emergence of influenza B viruses with reduced sensitivity to neuraminidase inhibitors. JAMA 297: 1435–1442.

14. Gubareva LV, Matrosovich MN, Brenner MK, Bethell RC, Webster RG (1998) Evidence for zanamivir resistance in an immunocompromised child infected with influenza B virus. J Infect Dis 178: 1257–1262.

15. Sugaya N, Mitamura K, Yamazaki M, Tamura D, Ichikawa M, et al. (2007) Lower clinical effectiveness of oseltamivir against influenza B contrasted with influenza A infection in children. Clin Infect Dis 44: 197–202.

16. Davies WL, Grunert RR, Haff RF, McGahen JW, Neumayer EM, et al. (1964) Antiviral Activity of 1-Adamantanamine (Amantadine). Science 144: 862–863.

17. De Clercq E (2006) Antiviral agents active against influenza A viruses. Nat Rev Drug Discov 5: 1015–1025.

18. Li ML, Rao P, Krug RM (2001) The active sites of the influenza cap-dependent endonuclease are on different polymerase subunits. EMBO J 20: 2078–2086.

19. Fechter P, Mingay L, Sharps J, Chambers A, Fodor E, et al. (2003) Two aromatic residues in the PB2 subunit of influenza A RNA polymerase are crucial for cap binding. J Biol Chem 278: 20381–20388.

20. Guilligay D, Tarendeau F, Resa-Infante P, Coloma R, Crepin T, et al. (2008) The structural basis for cap binding by influenza virus polymerase subunit PB2. Nat Struct Mol Biol 15: 500–506.

21. Dias A, Bouvier D, Crepin T, McCarthy AA, Hart DJ, et al. (2009) The cap-snatching endonuclease of influenza virus polymerase resides in the PA subunit. Nature 458: 914–918.

22. Yuan P, Bartlam M, Lou Z, Chen S, Zhou J, et al. (2009) Crystal structure of an avian influenza polymerase PA(N) reveals an endonuclease active site. Nature 458: 909–913.

23. Torreira E, Schoehn G, Fernandez Y, Jorba N, Ruigrok RW, et al. (2007) Three-dimensional model for the isolated recombinant influenza virus polymerase heterotrimer. Nucleic Acids Res 35: 3774–3783.

24. Coloma Ro, Valpuesta JM, Arranz Ro, Carrascosa JL, Ort√≠n J, et al. (2009) The Structure of a Biologically Active Influenza Virus Ribonucleoprotein Complex. PLoS Pathog 5: e1000491.

25. He X, Zhou J, Bartlam M, Zhang R, Ma J, et al. (2008) Crystal structure of the polymerase PA(C)-PB1(N) complex from an avian influenza H5N1 virus. Nature 454: 1123–1126.

26. Obayashi E, Yoshida H, Kawai F, Shibayama N, Kawaguchi A, et al. (2008) The structural basis for an essential subunit interaction in influenza virus RNA polymerase. Nature 454: 1127–1131.

27. Perez DR, Donis RO (1995) A 48-amino-acid region of influenza A virus PB1 protein is sufficient for complex formation with PA. J Virol 69: 6932–6939.

28. Perez DR, Donis RO (2001) Functional analysis of PA binding by influenza a virus PB1: effects on polymerase activity and viral infectivity. J Virol 75: 8127–8136.

29. Brownlee GG, Sharps JL (2002) The RNA polymerase of influenza a virus is stabilized by interaction with its viral RNA promoter. J Virol 76: 7103–7113.

30. Perales B, Ortin J (1997) The influenza A virus PB2 polymerase subunit is required for the replication of viral RNA. J Virol 71: 1381–1385.

31. Fodor E, Crow M, Mingay LJ, Deng T, Sharps J, et al. (2002) A single amino acid mutation in the PA subunit of the influenza virus RNA polymerase inhibits endonucleolytic cleavage of capped RNAs. J Virol 76: 8989–9001.

32. Ghanem A, Mayer D, Chase G, Tegge W, Frank R, et al. (2007) Peptide-mediated interference with influenza A virus polymerase. J Virol 81: 7801–7804.

33. Dostmann WR, Taylor MS, Nickl CK, Brayden JE, Frank R, et al. (2000) Highly specific, membrane-permeant peptide blockers of cGMP-dependent protein kinase Ialpha inhibit NO-induced cerebral dilation. Proc Natl Acad Sci U S A 97: 14772–14777.

34. Jambrina E, Barcena J, Uez O, Portela A (1997) The three subunits of the polymerase and the nucleoprotein of influenza B virus are the minimum set of viral proteins required for expression of a model RNA template. Virology 235: 209–217.

35. Crescenzo-Chaigne B, Naffakh N, van der Werf S (1999) Comparative analysis of the ability of the polymerase complexes of influenza viruses type A, B and C to assemble into functional RNPs that allow expression and replication of heterotypic model RNA templates in vivo. Virology 265: 342–353.

36. Iwatsuki-Horimoto K, Hatta Y, Hatta M, Muramoto Y, Chen H, et al. (2008) Limited compatibility between the RNA polymerase components of influenza virus type A and B. Virus Res 135: 161–165.

37. Wells JA, McClendon CL (2007) Reaching for high-hanging fruit in drug discovery at protein-protein interfaces. Nature 450: 1001–1009.

38. Berg T (2008) Small-molecule inhibitors of protein-protein interactions. Curr Opin Drug Discov Devel 11: 666–674.

39. Vassilev LT, Vu BT, Graves B, Carvajal D, Podlaski F, et al. (2004) In vivo activation of the p53 pathway by small-molecule antagonists of MDM2. Science 303: 844–848.

40. Berg T, Cohen SB, Desharnais J, Sonderegger C, Maslyar DJ, et al. (2002) Small-molecule antagonists of Myc/Max dimerization inhibit Myc-induced transformation of chicken embryo fibroblasts. Proc Natl Acad Sci U S A 99: 3830–3835.

41. Ambroise Y, Yaspan B, Ginsberg MH, Boger DL (2002) Inhibitors of cell migration that inhibit intracellular paxillin/alpha4 binding: a well-documented use of positional scanning libraries. Chem Biol 9: 1219–1226.

42. White PW, Titolo S, Brault K, Thauvette L, Pelletier A, et al. (2003) Inhibition of human papillomavirus DNA replication by small molecule antagonists of the E1-E2 protein interaction. J Biol Chem 278: 26765–26772.

43. Pilger BD, Cui C, Coen DM (2004) Identification of a small molecule that inhibits herpes simplex virus DNA Polymerase subunit interactions and viral replication. Chem Biol 11: 647–654.

44. Sugiyama K, Obayashi E, Kawaguchi A, Suzuki Y, Tame JR, et al. (2009) Structural insight into the essential PB1-PB2 subunit contact of the influenza virus RNA polymerase. EMBO J 28: 1803–1811.

45. Kosugi S, Hasebe M, Entani T, Takayama S, Tomita M, et al. (2008) Design of peptide inhibitors for the importin alpha/beta nuclear import pathway by activity-based profiling. Chem Biol 15: 940–949.

46. Munch J, Standker L, Adermann K, Schulz A, Schindler M, et al. (2007) Discovery and optimization of a natural HIV-1 entry inhibitor targeting the gp41 fusion peptide. Cell 129: 263–275.

47. Chokephaibulkit K, Uiprasertkul M, Puthavathana P, Chearskul P, Auewarakul P, et al. (2005) A child with avian influenza A (H5N1) infection. Pediatr Infect Dis J 24: 162–166.

48. Norton GP, Tanaka T, Tobita K, Nakada S, Buonagurio DA, et al. (1987) Infectious influenza A and B virus variants with long carboxyl terminal deletions in the NS1 polypeptides. Virology 156: 204–213.

49. Schwemmle M, Weining KC, Richter MF, Schumacher B, Staeheli P (1995) Vesicular stomatitis virus transcription inhibited by purified MxA protein. Virology 206: 545–554.

50. Pleschka S, Jaskunas R, Engelhardt OG, Zurcher T, Palese P, et al. (1996) A plasmid-based reverse genetics system for influenza A virus. J Virol 70: 4188–4192.

51. Schneider U, Naegele M, Staeheli P, Schwemmle M (2003) Active borna disease virus polymerase complex requires a distinct nucleoprotein-to-phosphoprotein ratio but no viral X protein. J Virol 77: 11781–11789.

52. Schmidtke M, Schnittler U, Jahn B, Dahse H, Stelzner A (2001) A rapid assay for evaluation of antiviral activity against coxsackie virus B3, influenza virus A, and herpes simplex virus type 1. J Virol Methods 95: 133–143.

53. Edgar RC (2004) MUSCLE: multiple sequence alignment with high accuracy and high throughput. Nucleic Acids Res 32: 1792–1797.